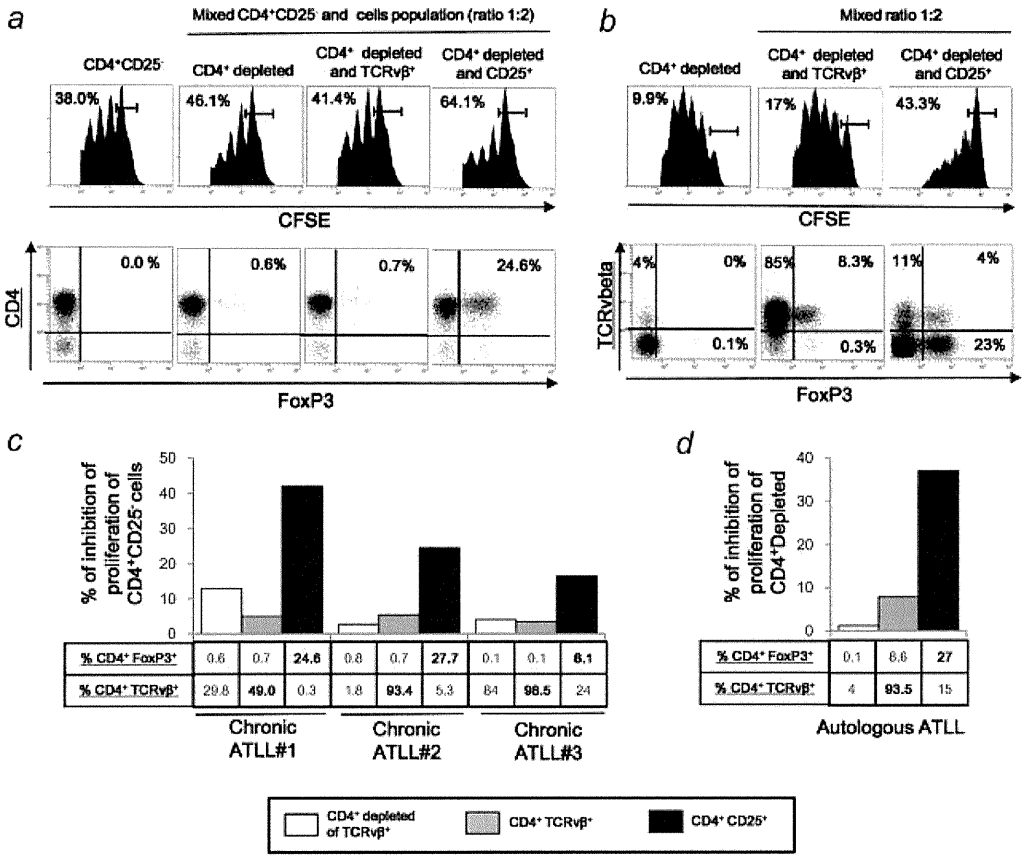

FIGURE 6 – Effect of $CD4^+TCRV\beta n^+$ clone and $CD4^+CD25^+FoxP3^+$ population on the proliferation of heterologous or autologous $CD4^+$ cells. We tested the ability of the $CD4^+TCRV\beta n^+$ or the $CD4^+CD25^+FoxP3^+$ population purified from PBMCs of patients with ATLL to inhibit the proliferation of either $CD4^+$-depleted cells from an uninfected individual (*b* and *c*) or autologous $CD4^+$-depleted ATLL cells (*d*). (*a*) Data on a representative patient with chronic ATLL. Each histogram represents the frequency of CFSE expression in $CD4^+$ cells isolated from uninfected cells, incubated for 4 days with the different cell populations indicated. The number in each histogram shows the percentage of undivided cells. The number in each scatter plot shows the frequency of expression of FoxP3 in the $CD4^+$ population. (*b*) Each histogram represents the frequency of CFSE expression in $CD4^+$ cells depleted of specific $TCRv\beta n^+$ and $CD25^+$ cells from autologous chronic ATLL patients. Cells were mixed with the different cell populations indicated and incubated for 4 days. The number in each histogram shows the percentage of undivided cells. The number in each scatter plot shows the frequency of expression of FoxP3 and specific $TCRv\beta n^+$ in the $CD4^+$ population. (*c* and *d*) Percentage of inhibition of $CD4^+$ T-cell proliferation, obtained using the following formula: [(% divided cells in control) − (% divided cells in sample)/(% divided cells in control)]. (*c*) Shows inhibition of proliferation of $CD4^+CD25^-$ cells from an uninfected individual; (*d*) shows inhibition of proliferation of autologous $CD4^+$ cells.

patient. Because we observed a saturation of the effect of $FoxP3^+$ cells on the inhibition of killing, we present the results on a logarithmic scale.

We observed a strong and statistically significant negative correlation between the frequency of FoxP3 expression and the rate of lysis of autologous $CD4^+Tax^+$ cells in unstimulated PBMCs from patients with ATLL (Fig. 7*a*). We also observed a significant negative correlation between the frequency of $CD4^+FoxP3^+Tax^-$ cells and the rate of CTL lysis (Fig. 7*b*). However, the frequency of the $CD4^+FoxP^+Tax^+$ population showed no correlation with the rate of lysis (data not shown).

Discussion

We report here 2 principal findings. First, our observations on patients with ATLL suggest that ATLL cells themselves are distinct from a functional $CD4^+FoxP3^+$ T_{reg} population. Second, in PBMCs from patients with ATLL, we detected a specific $CD8^+$ T-cell response to HTLV-1–expressing autologous lymphocytes, and this $CD8^+$ T-cell response was inversely correlated with the percentage of $CD4^+FoxP3^+$ cells.

ATLL cells characteristically express CD25 and CCR4 on the cell surface. Because ATLL cells in certain cases have also been found to express FoxP3, it has been suggested that the severe immune suppression characteristic of ATLL might result from a regulatory T-cell–like effect of ATLL cells. However, it was already established that Tax upregulates the expression of CD25 on infected cells, which complicates the attempt to identify T_{regs} in HTLV-1 infection.[16] In this study, we therefore chose to quantify expression of FoxP3, which is the best currently identified single marker of the main T_{reg} population.

Measurement of the frequency of FoxP3 expression in patients with ATLL and lymphoma showed that consistent with previous observations by others using RT-PCR to detect FoxP3 mRNA[10] patients with ATLL had a high frequency of FoxP3 expression in $CD4^+$ cells (Fig. 1*a*). As in our previous study of nonmalignant cases of HTLV-1 infection,[16] we distinguished 2 populations of $FoxP3^+$ cells in patients with ATLL: $CD4^+FoxP3^+Tax^+$ and $CD4^+FoxP3^+Tax^-$ cells. In patients with Tax^+ acute ATLL, we observed frequent coexpression of Tax and FoxP3 in $CD4^+$ cells (Fig. 3). The mean frequency of FoxP3 expression in the total $CD4^+$ population was lower in cases of acute ATLL than in chronic ATLL (Fig. 1*a*), although this difference was not statisti-

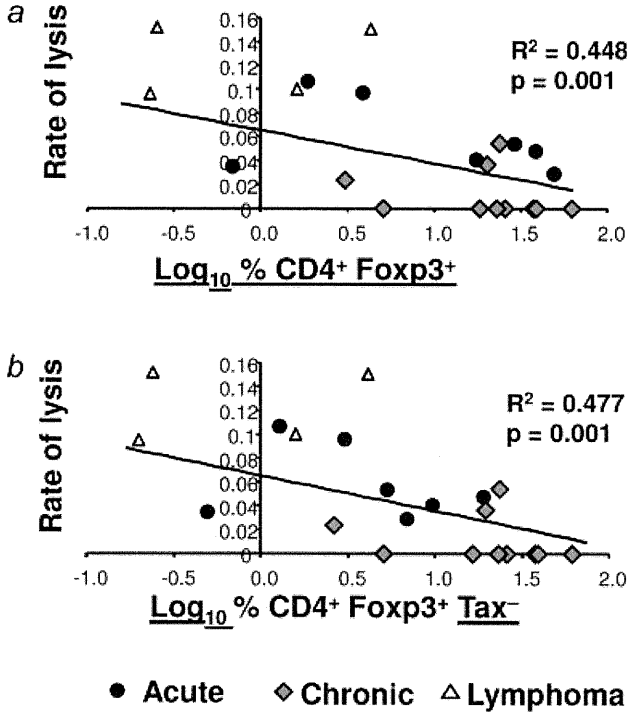

FIGURE 7 – FoxP3 control the CD8-mediated lysis against Tax^+ cells. Correlation between the rate of $CD8^+$ cell-mediated lysis of autologous Tax^+ cells in fresh PBMCs (rate of lysis) and (*a*) $\log_{10}$ (% $CD4^+FoxP3^+/CD4^+$) or (*b*) $\log_{10}$ (% $CD4^+FoxP3^+Tax^-/CD4$. *p* values were determined by a two-tailed Spearman test. Least-squares regression analysis showed (*e-g*, right-hand panels) a significant negative correlation between $\log_{10}$ (% $CD4^+FoxP3^+/CD4^+$) and the rate of $CD8^+$ cell-mediated lysis.

cally significant. Note that the cases of acute ATLL represented in Figure 1*a* are those whose PBMCs expressed detectable Tax protein. However, there was a clear distinction between these 2 subtypes of ATLL in the frequency of $CD4^+FoxP3^+$ cells in the Tax^- population (Fig. 3*c*): this frequency was significantly lower in patients with acute ATLL than in those with chronic ATLL. Furthermore, in acute ATLL, we observed a correlation between the frequency of expression of Tax and FoxP3, and cells from patients with acute ATLL that did not express Tax also did not express detectable FoxP3 (Fig. 3*d*). It remains unclear why this correlation was found among patients with acute ATLL but not in those with chronic ATLL. The positive correlation observed in acute ATLL patients was not simply caused by Tax-induced expression of FoxP3 in the infected cell because the frequency of Tax-expressing cells correlated independently with both the frequency of $FoxP3^+$ Tax^+ cells and the frequency of $FoxP3^+Tax^-$ cells (data not shown).

By observing FoxP3 and CD25 expression in patients with either chronic or acute ATLL, we found no correlation between the percentage of $CD4^+CD25^+$ cells and the percentage of $CD4^+FoxP3^+$ cells. This observation suggests that ATLL cells, which are almost invariably $CD25^+$, do not systematically express $FoxP3^+$ (Fig. 1*b*). This conclusion was reinforced by our observations on successive samples of PBMCs from 2 patients with chronic ATLL, in whom the frequency of ATLL cells varied substantially over years (Fig. 2). The first patient had a spontaneous remission; the second patient was initially asymptomatic, then the ATLL progressed and subsequently regressed after modification of treatment. In each of these 2 patients, we observed a variation in the absolute number of $CD4^+CD25^+$ cells that was independent of the number of $CD4^+FoxP3^+$ cells.

As an independent test of the expression of FoxP3 by ATLL cells, we used TCRVβ-specific antibodies to identify the ATLL clones in fresh PBMCs. Flow cytometric analysis of cells costained for CD4, FoxP3 and the respective TCRVβ chain (Fig. 5 and Supporting Information Data 1 and 2) confirmed that the chief $FoxP3^+$ cell population was distinct from the expanded $TCRV\beta n^+$ (ATLL) clones.

We wished to test the hypothesis that the $FoxP3^+$ cells observed in PBMCs from patients with ATLL exert immune suppressive effects typical of $FoxP3^+$ T_{reg} cells. We therefore studied the capacity of ATLL cells to inhibit proliferation of heterologous $CD4^+$ cells and the relationship of this inhibitory capacity to the frequency of $FoxP3^+$ expression (Fig. 4). We conclude that, even if the $CD25^+$ cells present in PBMCs in patients with ATLL exert an immune suppressive activity, this activity correlates with the frequency of $FoxP3^+$ expression. Moreover, we observed that the magnitude of inhibition of heterologous T-cell proliferation correlated with the frequency of $FoxP3^+$ Tax^- cells but not with the frequency of $FoxP3^+$ Tax^+ cells. These experiments indicate that the phenotype $FoxP3^+$ Tax^- remains a useful marker of T_{reg} function even in ATLL.

At present, it is not possible to specifically select $FoxP3^+$ cells and to conserve their functional properties because $FoxP3^+$ is a nuclear marker and unfixed cells therefore cannot be stained for FoxP3 expression. We therefore initially used the TCRVβ-specific antibodies to select the $TCRV\beta n^+$ ATLL clone and subsequently isolated the $CD25^+$ cells from the resulting $TCRV\beta n^+$-depleted population. In this way we enriched both the ATLL population and the $FoxP3^+$ population, respectively. The results (Fig. 6) showed that only the $FoxP3^+$ fraction caused strong inhibition of proliferation of $CD4^+$ cells from an uninfected patient (Figs. 6*b* and 6*c*) and of autologous $CD4^+$ cells (Fig. 6*d*). These experiments present further evidence of the presence of an independent functional FoxP3 population in patients with ATLL.

An HTLV-1–specific cell-mediated immune response in patients with ATLL has previously been reported by other groups.[21–23] Here, we used a recently developed method to quantify the CTL response against autologous Tax-expressing cells.[19] In addition, PBMCs from a proportion of patients with ATLL have been previously demonstrated to express HTLV-1 Tax protein after short-term incubation *in vitro*. In the present study, fresh PBMCs from all patients studied with chronic ATLL or lymphoma had detectable Tax expression. In contrast, Tax expression remained undetectable even after *in vitro* incubation for 18 hr in 5 of the 12 patients with acute ATLL. We next wished to test the hypothesis that the frequency of these different populations of $FoxP3^+$ cells was correlated with the rate of CTL-mediated lysis of Tax^+ cells measured in PBMCs from the patients with ATLL. We observed a strong negative correlation between the percentage of $CD4^+FoxP3^+$ cells and the rate of lysis (Fig. 7*a*). Furthermore, this correlation was stronger (*i.e.*, there was a larger value of R^2) with the $CD4^+FoxP3^+Tax^-$ population than with the total $CD4^+FoxP3^+$ population, and there was no significant correlation between the frequency of $CD4^+FoxP3^+Tax^+$ cells and the rate of lysis (Fig. 7*b*). This result suggests that the functional T_{reg} population consists of $CD4^+FoxP3^+Tax^-$ cells, whereas the $CD4^+FoxP3^+Tax^+$ cells do not appear to influence the CTL response to HTLV-1.

These observations indicate that the frequencies of functional Tax-FoxP3+Treg cells are lower in acute ATLL than in patients with chronic ATLL (Fig. 3*c*). Because we also demonstrate that the $FoxP3^+$ cells in ATLL are independent of the TCRVβ clone and retain the ability to inhibit the proliferation of $CD4^+$ T cells (Fig. 4), we hypothesize that the high frequency of $CD4^+FoxP3^+Tax^-$ cells with regulatory function observed in chronic ATLL contributes to the slow progression of the disease by suppressing ATLL cell proliferation.

This study suggests that ATLL cells themselves are distinct from a population of $FoxP3^+$ cells with functional characteristics of T_{regs}. Although the impact of the $FoxP3^+$ population on ATLL development and progression remains unclear, the present data

show that in patients with ATLL, a high frequency of $CD4^+FoxP3^+Tax^-$ cells is associated with a significant reduction in the rate of lysis of autologous HTLV-1-expressing cells, and with the capacity to suppress T-cell proliferation.

Acknowledgements

We thank Dr. Tao Dong for the gift of the anti-TCRVβ monoclonal antibodies.

References

1. Uchiyama T, Yodoi J, Sagawa K, Takatsuki K, Uchino H. Adult T-cell leukemia: clinical and hematologic features of 16 cases. Blood 1977;50:481–92.
2. Miyoshi I, Kubonishi I, Yoshimoto S, Akagi T, Ohtsuki Y, Shiraishi Y, Nagata K, Hinuma Y. Type C virus particles in a cord T-cell line derived by co-cultivating normal human cord leukocytes and human leukaemic T cells. Nature 1981;294:770–1.
3. Kalyanaraman VS, Sarngadharan MG, Nakao Y, Ito Y, Aoki T, Gallo RC. Natural antibodies to the structural core protein (p24) of the human T-cell leukemia (lymphoma) retrovirus found in sera of leukemia patients in Japan. Proc Natl Acad Sci U S A 1982;79:1653–7.
4. Kawano F, Yamaguchi K, Nishimura H, Tsuda H, Takatsuki K. Variation in the clinical courses of adult T-cell leukemia. Cancer 1985;55: 851–6.
5. Shimoyama M. Diagnostic criteria and classification of clinical subtypes of adult T-cell leukaemia-lymphoma. A report from the Lymphoma Study Group (1984–87). Br J Haematol 1991;79:428–37.
6. Akagi T, Ono H, Shimotohno K. Characterization of T cells immortalized by Tax1 of human T-cell leukemia virus type 1. Blood 1995;86: 4243–9.
7. Matsuoka M, Jeang KT. Human T-cell leukaemia virus type 1 (HTLV-1) infectivity and cellular transformation. Nat Rev Cancer 2007;7:270–80.
8. Roncador G, Garcia JF, Maestre L, Lucas E, Menarguez J, Ohshima K, Nakamura S, Banham AH, Piris MA. FOXP3, a selective marker for a subset of adult T-cell leukaemia/lymphoma. Leukemia 2005;19: 2247–53.
9. Chen S, Ishii N, Ine S, Ikeda S, Fujimura T, Ndhlovu LC, Soroosh P, Tada K, Harigae H, Kameoka J, Kasai N, Sasaki T, et al. Regulatory T cell-like activity of Foxp3+ adult T cell leukemia cells. Int Immunol 2006;18:269–77.
10. Kohno T, Yamada Y, Akamatsu N, Kamihira S, Imaizumi Y, Tomonaga M, Matsuyama T. Possible origin of adult T-cell leukemia/lymphoma cells from human T lymphotropic virus type-1-infected regulatory T cells. Cancer Sci 2005;96:527–33.
11. Bach JF. Regulatory T cells under scrutiny. Nat Rev Immunol 2003;3: 189–98.
12. Fontenot JD, Rudensky AY. A well adapted regulatory contrivance: regulatory T cell development and the forkhead family transcription factor Foxp3. Nat Immunol 2005;6:331–7.
13. Cross SL, Feinberg MB, Wolf JB, Holbrook NJ, Wong-Staal F, Leonard WJ. Regulation of the human interleukin-2 receptor alpha chain promoter: activation of a nonfunctional promoter by the transactivator gene of HTLV-I. Cell 1987;49:47–56.
14. Inoue J, Seiki M, Taniguchi T, Tsuru S, Yoshida M. Induction of interleukin 2 receptor gene expression by p40x encoded by human T-cell leukemia virus type 1. Embo J 1986;5:2883–8.
15. Ziegler SF. FOXP3: of mice and men. Annu Rev Immunol 2006;24: 209–26.
16. Toulza F, Heaps A, Tanaka Y, Taylor GP, Bangham CR. High frequency of CD4+FoxP3+ cells in HTLV-1 infection: inverse correlation with HTLV-1-specific CTL response. Blood 2008;111:5047–53.
17. Yano H, Ishida T, Inagaki A, Ishii T, Kusumoto S, Komatsu H, Iida S, Utsunomiya A, Ueda R. Regulatory T-cell function of adult T-cell leukemia/lymphoma cells. Int J Cancer 2007;120:2052–7.
18. Lee B, Tanaka Y, Tozawa H. Monoclonal antibody defining tax protein of human T-cell leukemia virus type-I. Tohoku J Exp Med 1989; 157:1–11.
19. Asquith B, Mosley AJ, Barfield A, Marshall SE, Heaps A, Goon P, Hanon E, Tanaka Y, Taylor GP, Bangham CR. A functional CD8+ cell assay reveals individual variation in CD8+ cell antiviral efficacy and explains differences in human T-lymphotropic virus type 1 proviral load. J Gen Virol 2005;86:1515–23.
20. Kannagi M, Harashima N, Kurihara K, Ohashi T, Utsunomiya A, Tanosaki R, Masuda M, Tomonaga M, Okamura J. Tumor immunity against adult T-cell leukemia. Cancer Sci 2005;96:249–55.
21. Kannagi M, Sugamura K, Kinoshita K, Uchino H, Hinuma Y. Specific cytolysis of fresh tumor cells by an autologous killer T cell line derived from an adult T cell leukemia/lymphoma patient. J Immunol 1984;133:1037–41.
22. Arnulf B, Thorel M, Poirot Y, Tamouza R, Boulanger E, Jaccard A, Oksenhendler E, Hermine O, Pique C. Loss of the ex vivo but not the reinducible CD8+ T-cell response to Tax in human T-cell leukemia virus type 1-infected patients with adult T-cell leukemia/lymphoma. Leukemia 2004;18:126–32.
23. Harashima N, Kurihara K, Utsunomiya A, Tanosaki R, Hanabuchi S, Masuda M, Ohashi T, Fukui F, Hasegawa A, Masuda T, Takaue Y, Okamura J, et al. Graft-versus-Tax response in adult T-cell leukemia patients after hematopoietic stem cell transplantation. Cancer Res 2004;64:391–9.

JOURNAL OF VIROLOGY, July 2010, p. 7278–7287 Vol. 84, No. 14
0022-538X/10/$12.00 doi:10.1128/JVI.02239-09

APOBEC3G Generates Nonsense Mutations in Human T-Cell Leukemia Virus Type 1 Proviral Genomes *In Vivo*▽†

Jun Fan,[1] Guangyong Ma,[1] Kisato Nosaka,[2] Junko Tanabe,[1] Yorifumi Satou,[1] Atsushi Koito,[3] Simon Wain-Hobson,[4] Jean-Pierre Vartanian,[4] and Masao Matsuoka[1]*

Laboratory of Virus Control, Institute for Virus Research, Kyoto University, 53 Shogoin Kawahara-cho, Sakyo-ku, Kyoto 606-8507, Japan[1]; Department of Hematology and Infectious Diseases, Kumamoto University School of Medicine, 1-1-1 Honjo, Kumamoto 860-0811, Japan[2]; Department of Retrovirology and Self-Defense, Faculty of Medical and Pharmaceutical Sciences, Kumamoto University School of Medicine, 1-1-1 Honjo, Kumamoto 860-0811, Japan[3]; and Molecular Retrovirology Unit, Institut Pasteur, 28 rue du Dr. Roux 75724 Paris Cedex 15, France[4]

Received 23 October 2009/Accepted 23 April 2010

Human T-cell leukemia virus type 1 (HTLV-1) induces cell proliferation after infection, leading to efficient transmission by cell-to-cell contact. After a long latent period, a fraction of carriers develop adult T-cell leukemia (ATL). Genetic changes in the *tax* gene in ATL cells were reported in about 10% of ATL cases. To determine genetic changes that may occur throughout the provirus, we determined the entire sequence of the HTLV-1 provirus in 60 ATL cases. Abortive genetic changes, including deletions, insertions, and nonsense mutations, were frequent in all viral genes except the *HBZ* gene, which is transcribed from the minus strand of the virus. G-to-A base substitutions were the most frequent mutations in ATL cells. The sequence context of G-to-A mutations was in accordance with the preferred target sequence of human APOBEC3G (hA3G). The target sequences of hA3G were less frequent in the plus strand of the *HBZ* coding region than in other coding regions of the HTLV-1 provirus. Nonsense mutations in viral genes including *tax* were also observed in proviruses from asymptomatic carriers, indicating that these mutations were generated during reverse transcription and prior to oncogenesis. The fact that hA3G targets the minus strand during reverse transcription explains why the *HBZ* gene is not susceptible to such nonsense mutations. HTLV-1-infected cells likely take advantage of hA3G to escape from the host immune system by losing expression of viral proteins.

Human T-cell leukemia virus type 1 (HTLV-1) is the causative agent of both adult T-cell leukemia (ATL) and inflammatory HTLV-1-associated myelopathy/tropical spastic paraparesis (HAM/TSP) (9, 40). HTLV-1 is a complex retrovirus that carries regulatory genes, such as *tax* and *rex*, and accessory genes, such as *p12*, *p13*, and *p30* (6, 29). An accessory gene, *HTLV-1 bZIP factor* (*HBZ*), is transcribed from the 3′ long terminal repeat (3′LTR) as an antisense transcript (10, 46). Previous studies have shown that Tax expression can immortalize T lymphocytes *in vitro* (1, 11), and *in vivo* the expression of Tax in transgenic mice causes various tumors depending on the tissue-specific promoter that expresses Tax (12, 14, 20). In more than half of human ATLs, the *tax* gene is not transcribed (41). Three mechanisms have been identified to inactivate Tax expression (29): (i) abortive genetic changes in the *tax* gene (7, 41), (ii) silencing by DNA methylation in the 5′LTR (18, 43), and (iii) deletion of the 5′LTR (31, 42). Since Tax is a major target of cytotoxic T-lymphocytes (CTLs) *in vivo* (17), the tumor cells might escape from the host immune system by suppressing Tax expression. However, the actual mechanism used to create genetic changes in the *tax* gene remains to be elucidated. Nonsense mutations in the *tax* gene have also been observed in HTLV-1 carriers, and the mechanism to generate these mutations is similarly unknown (8).

As a host defense against retroviruses, mammalian cells employ the APOBEC3 cytidine deaminase family, which causes deamination during reverse transcription, resulting in nucleotide mutations (3, 26). Human APOBEC3G (hA3G) deaminates cytosine residues of single-stranded DNA during reverse transcription, resulting in high levels of plus-strand G-to-A mutations. The human immunodeficiency virus (HIV) nucleocapsid is critical for incorporation of hA3G into virions (2, 24), while its accessory protein, Vif, counteracts hA3G. Vif inhibits hA3G packaging into HIV-1 virion through ubiquitination and proteasomal degradation of hA3G (39, 49). HTLV-1 does not encode a protein analogous to Vif that inactivates hA3G. Instead, it has been demonstrated that a domain of the HTLV-1 nucleocapsid suppresses the incorporation of hA3G into the virion (4). Consistent with this finding, it has been reported that G-to-A mutations are rare in HTLV-1 carriers (25).

In this study, we analyzed the entire sequences of proviruses in ATL and carrier cells and found that most nonsense mutations in the proviruses were caused by deamination. The sites of nonsense mutation coincided with the preferred target sequences of hA3G. In ATL cells, nonsense mutations, deletions, and insertions were detected in most of the viral genes except the *HBZ* gene, supporting the critical role of the *HBZ* gene in ATL.

* Corresponding author. Mailing address: Institute for Virus Research, Kyoto University, 53 Shogoin Kawahara-cho, Sakyo-ku, Kyoto 606-8507, Japan. Phone: 81-75-751-4048. Fax: 81-75-751-4049. E-mail: mmatsuok@virus.kyoto-u.ac.jp.

† Supplemental material for this article may be found at http://jvi.asm.org/.

▽ Published ahead of print on 12 May 2010.

MATERIALS AND METHODS

Cell lines and clinical samples. MT-2 and MT-4 are HTLV-1-transformed cell lines. MT-1 and TL-Om1 were derived from leukemia cells. Jurkat cells were negative for HTLV-1. These cells were cultured in RPMI 1640 medium supplemented with 10% fetal bovine serum, 100 U/ml penicillin, 100 μg/ml streptomycin, and 2 mM L-glutamine at 37°C in a 5% CO_2 atmosphere. Clinical samples were collected from 60 ATL patients and 10 HTLV-1 carriers. Genomic DNA was extracted from peripheral blood mononuclear cells using standard phenol-chloroform methods. This study was conducted according to the principles regarding human experimentation expressed in the Declaration of Helsinki. The study was approved by the Institutional Review Board of Kyoto University (G204). All patients provided written informed consent for the collection of samples and subsequent analysis.

Sequencing the complete provirus genomes in ATL cells. The copy number of HTLV-1 provirus in cells from ATL patients was determined by inverse PCR (5), and ATL samples with one complete provirus were selected for direct sequencing. The complete provirus genome was amplified as two halves (fragments I and II) from genomic DNA samples derived from ATL patients. Fragment I was amplified using primers 5′-TGACAATGACCATGAGCCCCAAATATCC-3′ and 5′-CGGCTATTAAGACCAGGAAG-3′. PCR conditions were as follows: an initial step of 5 min at 94°C; 30 cycles, with 1 cycle consisting of 30 s at 94°C, 30 s at 64°C, and 5 min at 72°C; and a final step of 10 min at 72°C. Fragment II was amplified using primers 5′-AGAAACAAGCTCAGAAGCTA-3′ and 5′-TGTACTAAATTTCTCTCCTGAGAGTGC-3′. PCR conditions were as follows: an initial step of 5 min at 94°C; 30 cycles, with 1 cycle consisting of 30 s at 94°C, 30 s at 60°C, and 5 min at 72°C; and a final step of 10 min at 72°C. PCR products were then subjected to nested PCR to amplify I-1 and I-2 from fragment I and II-1 and II-2 from fragment II. The primers for I-1 were 5′-TGACAATGACCATGAGCCCCAAATATCC-3′ and 5′-GAGCTTAAAGTGATCTTGG-3′. The primers for I-2 were 5′-TTCCGATAGCCTTGTTCTCA-3′ and 5′-CGGCTATTAAGACCAGGAAG-3′. The primers for II-1 were 5′-TGGTATTATTTCAAGCTTCC-3′ and 5′-AAATGCAGGAGTTGGGGATT-3′. The primers for II-2 were 5′-AACTGTCTAGTATAGCCATC-3′ and 5′-TGTACTAAATTTCTCTCCTGAGAGTGC-3′. PCR conditions for nested PCR were as follows: an initial step of 5 min at 94°C; 28 cycles, with 1 cycle consisting of 30 s at 94°C, 30 s at X°C, and 2.5 min at 72°C; and a final step of 72°C for 10 min. X was 60°C for I-1 and II-2 and 58°C for I-2 and II-1. The final PCR products were gel purified, and the sequence was determined by direct sequencing.

Sequencing the *pol* and *tax* regions in HTLV-1 carriers. The proviral load was determined as previously reported (32). Herculase II fusion DNA polymerase (Stratagene, La Jolla, CA), a *Pfu*-based DNA polymerase, was used to amplify *pol* and *tax* regions from genomic DNA derived from HTLV-1 carriers. The primers used to amplify the *pol* region were 5′-TACACCTTGCAATCCTATGG-3′ and 5′-GCTAGGCTTGCCTAGATGGG-3′. PCR conditions were as follows: an initial step of 5 min at 95°C; 30 cycles, with 1 cycle consisting of 20 s at 95°C, 20 s at 60°C, and 50 s at 72°C; and a final step of 50 s at 72°C. The primers used to amplify the *tax* region were 5′-GGTCCTCCGGGCATGACACA-3′ and 5′-TCTCCACGCTTTTATAGACT-3′. PCR conditions were as follows: an initial step of 5 min at 95°C; 28 cycles, with 1 cycle consisting of 20 s at 95°C, 20 s at 68°C, and 50 s at 72°C; and a final step of 5 min at 72°C. The PCR products were purified and cloned, and at least 20 clones were sequenced. DNA polymerase fidelity was studied by using a clone carrying an amplified *tax* region as the template instead of genomic DNA. The *tax* region was amplified using the same PCR conditions described above and cloned, and 25 clones were sequenced.

Sequencing the HTLV-1 genome in nontumor cells derived from ATL samples. ATL patient-derived tumor cells are considered a mixture of a major population of monoclonal expanded tumor cells and a minor population of HTLV-1-infected nontumor cells. To amplify the HTLV-1 genome from infected nontumor cells, ATL samples carrying defective HTLV-1 genome based on direct sequencing were selected. Target regions were amplified by setting one of the primers at the deleted region. Sequences were determined by direct sequencing.

Mutation analysis. Nucleotide sequences of all ATL samples were aligned using GENETYX-MAC version 13.0 software. Mutations were determined after filtering for (i) polymorphisms, defined as a nucleotide substitution occurring in >5 cases; and (ii) linkers, defined as >7 common nucleotide substitutions occurring in >2 cases. With these criteria, the nucleotide sequence from an ATL case, ATL-25, showed the fewest mutations (3 single-nucleotide substitutions with no deletions or insertions) and was selected as a standard sequence (AB513134). The nucleotide positions of identified mutations were numbered relative to this standard sequence.

For carrier samples, the sequence of a given region from all clones amplified from a carrier was aligned and compared with the standard sequence described above with mutated bases corrected. When a nucleotide substitution occurred in all clones, it was considered a polymorphism and excluded from the mutation repertoire.

cDNA synthesis and quantitative real-time RT-PCR. Total RNA was extracted from transfectants using Trizol reagent (Invitrogen, Carlsbad, CA). RNA was treated with DNase I (Invitrogen) to eliminate the genomic DNA. cDNA was synthesized from 1 μg of total RNA with the Superscript preamplification system (Invitrogen) according to the manufacturer's protocol. cDNA product was quantified by real-time reverse transcription-PCR (RT-PCR) with power SYBR green PCR master mix and 7900HT fast real-time PCR system (both from Applied Biosystems) according to the manufacturer's instructions. The specific primers for the *hA3G* gene were 5′-CGCGTGCCACCATGAAGATC-3′ (forward) and 5′-TGTGGGTGGATCCATCGAGT-3′ (reverse). The specific primers for the human *AID* gene were 5′-TTCACCGCGCGCCTCTACTT-3′ (forward) and 5′-GCTGTCTGGAGAGACGAACT-3′ (reverse). Target cDNA was normalized to the amount of endogenous mRNA of *ACTB*. The primers used for *ACTB* were 5′-AGGCCAACCGCGAGAAGATG-3′ (forward) and 5′-CCAGAGGCGTACAGGGATAG-3′ (reverse). PCRs were carried out in triplicate. Data were analyzed by the comparative threshold cycle (C_T) method according to protocols of the manufacturer (Applied Biosystems).

***In vitro* editing of the HTLV-1 genome by hA3G.** QT6 quail cells were transfected with an infectious molecular clone of HTLV-1 (pX1MT-M) (30) in the presence or absence of the hA3G expression plasmid. Twenty-four hours post-transfection, HTLV-1-producing QT6 cells were treated with 200 μg/ml of mitomycin C at 37°C for 30 min, washed well, and then cocultivated 1:1 with fresh QT6 cells (13). Seventy-two hours later, the cells were collected, and genomic DNA was extracted. hA3G-mediated DNA hypermutation was detected using three-dimensional (3D) PCR that allows differential amplification of G-to-A hypermutants using a *Taq* DNA polymerase as previously described (25). The first round of PCR was performed with a denaturation temperature of 94°C using the primer pair 5′-CTGCAGATACAAAGTTAACC-3′ (forward) and 5′-TGGAGGAAGGAGGGTGGAAT-3′ (reverse). PCR conditions were as follows: an initial step of 5 min at 94°C; 35 cycles, with 1 cycle consisting of 30 s at 94°C, 30 s at 58°C, and 30 at 72°C; and a final extension step of 10 min at 72°C. Then, 0.5 μl of the first-round reaction product was used as the template for the second round of PCR using the following primers: 5′-CCATGCTTATTATCAGCCCA-3′ (forward) and 5′-GTTGGGGGTTGTATGAGTGA-3′ (reverse). The PCR program was the same as for the first round of reaction except that the denaturation gradient ranged from 94 to 82°C. PCR products were purified and cloned, and up to 20 clones were sequenced.

Nucleotide sequence accession number. The nucleotide sequence of ATL-25, selected as the standard sequence, has been submitted to the DDBJ (DNA Data Bank of Japan) database under accession number AB513134.

RESULTS

HTLV-1 proviral sequence changes in ATL. Previous studies showed that Tax expression was frequently lost by genetic changes in the *tax* gene, by DNA methylation of the 5′LTR, and by deletion of the 5′LTR (29). Similarly, although not well studied thus far, the expression of other viral proteins might also be lost through genetic changes in the provirus sequence. To analyze the genetic changes of the HTLV-1 provirus in ATL cells, we determined the entire sequence of the provirus (9,034 bp) in 60 ATL cases. For this study, we chose ATL cases with HTLV-1 proviruses containing both LTRs. As shown in Table 1, we detected genetic changes (nonsense mutations, deletions, and insertions) in the coding regions of viral genes in 28 of 60 ATL cases (46.7%). Deletions in the proviruses were detected in 27 cases (45%), while insertions were found in 10 cases (16.7%) (see Table S1 in the supplemental material). These deletions and insertions resulted in the loss or truncation of protein(s) in 18 cases (Table 1; also see Table S1 in the supplemental material).

Nonsense mutations, deletions, and insertions in the viral genes were found in all viral genes except the *HBZ* gene (Table 1). Since the *p30* and *p13* genes use an identical coding frame, the same mutations generate nonsense changes in both *p30*

TABLE 1. Abortive genetic changes of HTLV-1 viral genes in 60 ATL cases[a]

ATL case	Genetic change[b] in the following viral gene:								
	gag	*pol*	*env*	*p12*	*p30*	*p13*	*p27*	*tax*	*HBZ*
ATL-2		DEL							
ATL-3								W248*	
ATL-7			DEL						
ATL-8			DEL				W139*		
ATL-10	DEL	DEL	DEL						
ATL-11		W680*	W427*						
ATL-12	DEL		W387*		W165*	W11*	W139*	W56*	
ATL-13	W59*	W680*	DEL		W165*	W11*		W56*	
					W190*	W36*			
ATL-14							DEL	DEL	
ATL-15		W680*							
ATL-27		DEL							
ATL-29			W431*		W165*	W11*		W56*	
ATL-32		W271*							
ATL-36								DEL	
ATL-37		W485*	W50*					W56*	
		W680*							
ATL-39				W87*					
ATL-40					R184*	R30*			
ATL-41		W485*						W56*	
ATL-42			DEL						
ATL-43		DEL							
ATL-44	DEL	DEL		W87*					
ATL-45	DEL							Y286*	
ATL-46	DEL	DEL							
ATL-47	DEL	DEL							
ATL-48	DEL							IN	
ATL-49	DEL	DEL							
ATL-51					W178*	W24*			
ATL-53	DEL								

[a] Only ATL cases with deletions, insertions, or nonsense mutations are shown.
[b] Abbreviations: DEL, deletion; IN, insertion; W, tryptophan; R, arginine; Y, tyrosine. A number after an amino acid indicates the position of the nonsense mutation. Stop codons are indicated by an asterisk.

and *p13* (Fig. 1). The frequency of genetic changes in the *tax* gene was 16.7% (10/60) (Table 1), which was higher than in previous studies (7, 41). Of a total of 29 nonsense mutations, 27 preferentially accumulated in tryptophan codons (27/29 [93.1%]) (see Table S2 in the supplemental material). Since the tryptophan codon is TGG, a G-to-A mutation generates either a TGA or a TAG stop codon. In one nonsense mutation, the codon for arginine (CGA) was converted to the TGA stop codon by a C-to-T mutation. Interestingly, nonsense mutations tended to accumulate in the same cases (Table 1).

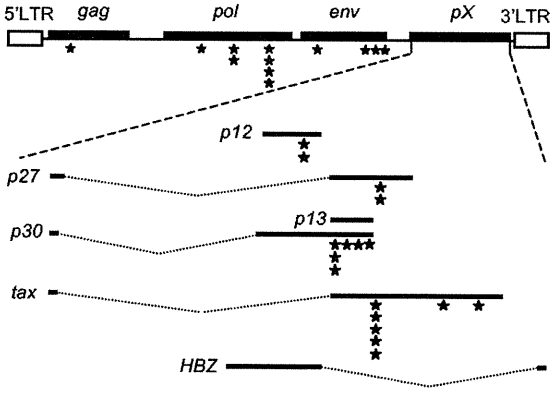

FIG. 1. Schema of the distribution of nonsense mutations in the HTLV-1 provirus. The *p13* gene has the same reading frame as the *p30* gene. Nonsense mutations observed in ATL cases are indicated by black stars.

It was difficult to discriminate between mutations and polymorphisms in HTLV-1 provirus from ATL patients, since the proviral sequences in nonleukemic cells could not be analyzed in most ATL cases without an internal deletion of provirus. Some mutations might be characteristic of a subgroup of proviruses (polymorphism). Since nonsense mutations at the *tax* gene (nucleotide position 7469) were detected in 5 ATL cases, we tentatively classified base substitutions as polymorphisms when more than 5 identical base substitutions were observed in different cases. On the basis of this criterion, we observed 591 mutations in all ATL cases (see Table S3 in the supplemental material). Among them, the G-to-A mutation was the most frequent, contributing to 28.8% of the total mutations. Other frequently detected mutations were the C-to-T (23.7%), A-to-G (17.1%), and T-to-C (12.9%) mutations. Frequent G-to-A and C-to-T mutations strongly suggested the activity of deamination enzymes in the generation of these mutations.

Mutations in leukemic and nonleukemic cells in ATL cases. In ATL patients, nonleukemic HTLV-1-infected cells coexist with leukemic cells. To analyze the proviral sequences of nonleukemic cells, we amplified proviral sequences using primers within regions deleted in leukemic cells to avoid amplification of provirus from leukemic cells. Nonsense mutations that were

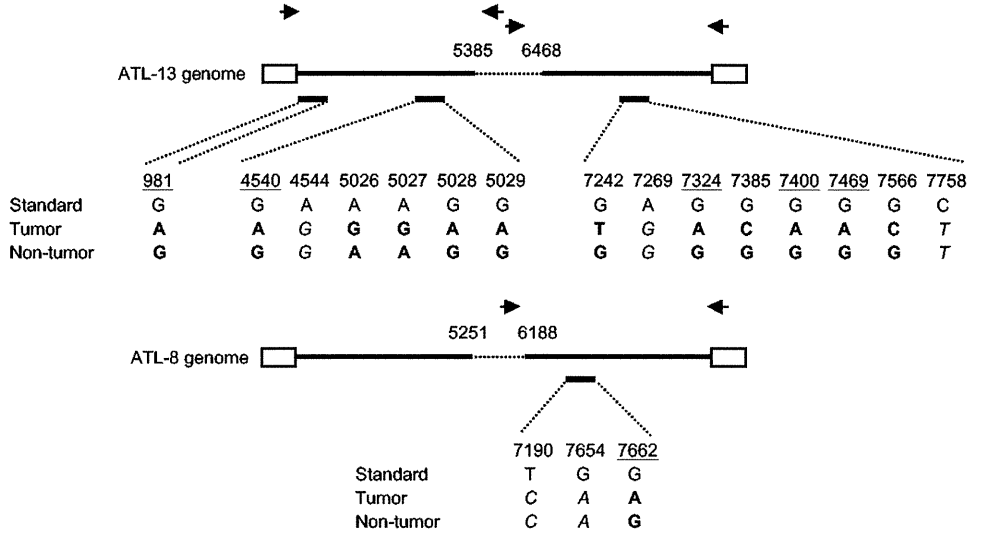

FIG. 2. Mutations in non-tumor-cell-derived proviral sequence in ATL patients. HTLV-1 genomes with internal deleted regions from two samples from two ATL patients are displayed schematically. As indicated by horizontal arrows, one of the PCR primers was set in the deleted region in order to specifically amplify a proviral region that originated from nontumor cells (see Materials and Methods). Nested PCR products, represented by short black lines, were subjected to direct sequencing. Nucleotide bases mutated in tumor cells according to the criteria mentioned in Materials and Methods are displayed. A base substitution is considered a polymorphism if the same base was found also in the nontumor cells derived from the same patient sample. Positions at which a G-to-A mutation will result in a nonsense mutation are underlined.

observed in leukemic cells were not detected in nonleukemic cells (Fig. 2), indicating that nonsense mutations generated in the provirus of leukemic cells were selected for. We compared the entire sequence of the HTLV-1 provirus in both leukemic cells and nonleukemic cells from five ATL cases. As shown in Table 2, only 37% of base substitutions were considered real mutations, since the nucleotide differed between leukemic cells and nonleukemic cells. However, 71% of G-to-A transitions were actually mutations, while 73% of other base substitutions were polymorphisms (Table 2), indicating that G-to-A mutations are predominant in ATL cells.

Association of G-to-A mutations with human APOBEC3G. A high frequency of G-to-A mutations suggests the role of deaminase(s) in generating these mutations. Deamination enzymes are known to have individually preferred target sequences for deamination (44). Sequences surrounding the nonsense mutations generated by the G-to-A mutation in HTLV-1 proviruses showed a predominance of the 5′-GG dinucleotide context (target underlined) (Fig. 3A). Among trinucleotides containing GG dinucleotides, CGG, TGG, and GGG were preferred (Fig. 3A); these are consistent with the target sequences of human APOBEC3G (hA3G) (48). The AGG sequence was also targeted in HTLV-1, unlike HIV-1. When we checked tetrameric sequences that contain a central GG dinucleotide, CGGG and TGGG were the preferred targets in the HTLV-1 provirus, similar to those reported for HIV-1 (Fig. 3B). As in HIV-1, a C at the +2 position (NGGC [N indicates T or C]) was not favored in HTLV-1. These findings suggest that the observed G-to-A mutations were generated by hA3G. Another deaminase, human APOBEC3F (hA3F), which is largely coexpressed with hA3G, is also reported to target single-stranded minus-strand DNA (46). Unlike hA3G, which favors the 5′-GG dinucleotide, the consensus target sequence of hA3F is 5′-GA (21). G-to-A mutations at GA sites contributed 13.4% of all G-to-A mutations (Fig. 3A), suggesting that hA3F might also play a role in these mutations in the HTLV-1 provirus.

Since hA3G targets the minus strand during reverse tran-

TABLE 2. Concordance rate of mutations between leukemic cells and nonleukemic cells in five ATL cases

ATL case or parameter	No. of mutations[a]												
	Total[b]	G-to-A	C-to-T	A-to-G	T-to-C	A-to-C	A-to-T	C-to-G	C-to-A	T-to-G	G-to-C	G-to-T	T-to-A
ATL-8	10 (4)	2 (1)	3 (1)	2 (0)	1 (0)			1 (1)			1 (1)		
ATL-12	25 (8)	8 (6)	7 (2)	5 (0)	3 (0)			2 (0)					
ATL-13	36 (20)	10 (8)	8 (3)	7 (2)	2 (1)	2 (0)			1 (0)	1 (0)	3 (3)	1 (0)	1 (0)
ATL-14	12 (2)	1 (1)	7 (0)	1 (0)	2 (0)				1 (1)				
ATL-45	16 (3)	3 (1)	3 (0)	4 (0)	2 (1)		3 (0)		1 (1)				
Total	99 (37)	24 (17)	28 (6)	19 (2)	10 (2)	2 (0)	3 (0)	3 (1)	3 (2)	1 (0)	4 (4)	1 (0)	1 (0)
Concordance rate (%)	37	71	21	11	20	0	0	33	67	0	100	0	0

[a] Each entry [*A* (*B*)] shows the number of each type of mutation in ATL cases judged by our criteria (*A*) and the number of confirmed mutations (*B*). The concordance rate of mutations was calculated by dividing *B* by *A*.
[b] Number of mutations of all types in each ATL case.

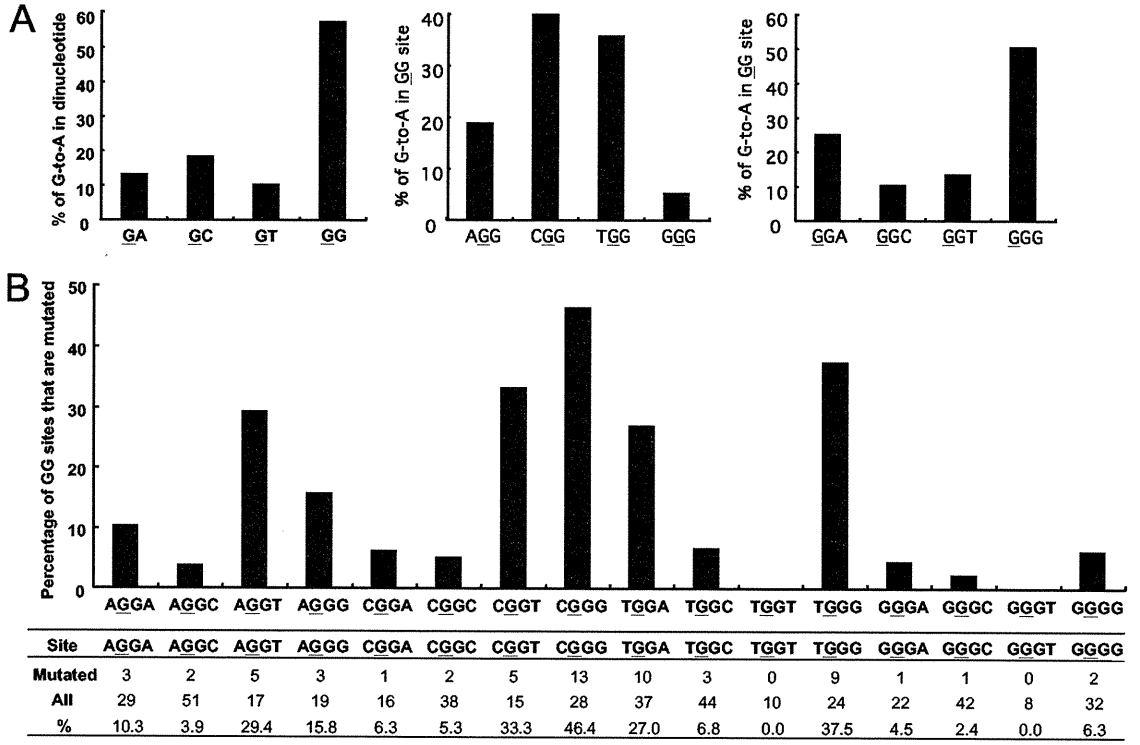

Site	AGGA	AGGC	AGGT	AGGG	CGGA	CGGC	CGGT	CGGG	TGGA	TGGC	TGGT	TGGG	GGGA	GGGC	GGGT	GGGG
Mutated	3	2	5	3	1	2	5	13	10	3	0	9	1	1	0	2
All	29	51	17	19	16	38	15	28	37	44	10	24	22	42	8	32
%	10.3	3.9	29.4	15.8	6.3	5.3	33.3	46.4	27.0	6.8	0.0	37.5	4.5	2.4	0.0	6.3

FIG. 3. Target sequence preference of G-to-A mutations. (A) Sequence context of G-to-A mutations. In all G-to-A mutations, the percentage of mutations at the indicated dinucleotide sequence context is shown (left panel). In the GG context, the influence of 5′ (middle panel) and 3′ (right panel) nucleotides neighboring the GG dinucleotide on G-to-A mutations is displayed. (B) Frequency of G-to-A mutations on sites of tetranucleotides containing a central GG. HTLV-1 genome sequence from ATL-25 was used as a standard sequence with mutated bases corrected to calculate the total number of GG sites that exist in the provirus genome (see Materials and Methods). The percentage of GG sites that underwent G-to-A mutation at least once in 60 ATL cases was plotted against each sequence context. Mutated bases are underlined. CGGG and TGGG were the preferred targets for G-to-A mutation in the HTLV-1 provirus. A C at position +2 (NGGC) was not favored.

scription, nonsense mutations generated by G-to-A mutations are not found in the *HBZ* gene. A G-to-A mutation in the proviral sense strand caused a nonsense mutation in the *p12* gene (TGG to TGA), whereas the same mutation generated a missense mutation in the *HBZ* gene (CCA to TCA) (Fig. 1). G-to-A mutations occurred most frequently at GG sites (target underlined) with a T or C at their 5′ terminus (Fig. 3A). We therefore counted the number of TGG or CGG sites within individual HTLV-1 regions (Table 3). As NGGC (N indicates T or C) was not favored by hA3G (Fig. 3B), it was not included. Among HTLV-1 regions, the plus-strand sequence of the *HBZ* gene had the fewest TGG and CGG sites, even when the number of sites was normalized by the size of the region. This indicates that mutations in the *HBZ* gene-coding region caused by hA3G are also rare.

TABLE 3. Distribution of hA3G target sequence in the plus strand of the HTLV-1 genome

Gene or genome region	Size (bp)	No. of sites[a]			
		CGGX	CGGX/kb	TGGX	TGGX/kb
5′LTR	755	8	10.60	3	3.97
gag	1,290	12	9.3	10	7.75
pol	2,691	16	5.95	25	9.29
env	1,467	8	5.45	17	11.59
p27	570	3	5.26	10	17.54
p30	726	2	2.75	7	9.64
tax	1,062	5	4.71	11	10.36
HBZ	621	1	1.61	1	1.61
3′LTR	755	7	9.27	3	3.97

[a] Number of sites (e.g., CGGX sites or TGGX sites, where X indicates A, T, or G) alone or the number of CGGX or TGGX sites normalized by the size of the region (e.g., number of CGGX sites in 1 kb [CGGX/kb]).

Mutations in the HTLV-1 proviral sequences from carriers. Frequent detection of G-to-A mutations in HTLV-1 proviral sequences in ATL cases suggests that these nonsense mutations potentially occur in both HTLV-1 carriers and ATL patients. To explore this possibility, we next studied the proviral sequences of the *pol*, *env*, *p12*, *p13/p30*, *p27*, *tax*, and *HBZ* genes in asymptomatic HTLV-1 carriers. The proviral sequences in asymptomatic carriers were amplified using a high-fidelity DNA polymerase with proofreading activity, and after subcloning, the sequences were determined for at least 20 subclones. As seen in ATL cases, the mutation frequency differed drastically among individual carriers (representative data are shown in Tables S4 and S5 in the supplemental material), and the distribution of base substitutions among clones varied within individual carriers. G-to-A mutations accounted for 81% and 72% of all mutations in the *pol* and *tax* genes, respectively (Table 4 and 5, respectively). A high frequency of G-to-A mutations was also observed in other viral genes (data not shown). Analyses of the sequence context of G-to-A mutations showed a predominance of GG sequences, which is

TABLE 4. Mutations in the *pol* region of 10 HTLV-1 carriers

HTLV-1 carrier (no. of clones)[a]	No. of the indicated single-nucleotide substitution in HTLV-1 carrier:									No. of sequences with the following sequence context for the G-to-A mutation[b]:			
	G-to-A	C-to-T	A-to-G	T-to-C	A-to-C	C-to-G	G-to-C	G-to-T	T-to-A	GA	GC	GT	GG
C72 (25)	5	1					1						5
C79 (20)	8		1		1			1		1	1		6
C63 (28)	1							1				1	
C40 (26)	13		1										13
C32 (22)		2											
C62 (22)	1	2											1
C87 (22)	14									1	1		13
C5 (23)	19	1						1	2				19
C29 (25)	9					1		1			1		8
C82 (27)	7			1							1		6
Total	77	6	2	1	1	1	1	4	2	2	4	1	71

[a] The number of clones studied from each carrier is shown in parentheses.
[b] Mutated bases are underlined.

consistent with the finding that hA3G deaminates the viral genome during reverse transcription (48). In order to compare the frequencies of nonsense mutations in carriers versus ATL cases, the occurrence of nonsense mutations was further analyzed. Consistent with the findings for ATL cases, nonsense mutations were detected in the *pol*, *env*, *p30/p13*, *p27*, and *tax* genes, but not in the *p12* and *HBZ* genes (Table 6). As in ATL cases, nonsense mutations in carriers were most frequently observed in the *tax* and *pol* genes. This result suggests that there is no bias for mutations in specific viral genes in ATL cases compared with carriers. These results suggest that nonsense mutations in provirus are not generated during oncogenesis but are present in the carrier state.

In addition to G-to-A mutations, C-to-T mutations were detected in the *pol* and *tax* genes in carrier cells as in ATL cells (see Table S2 in the supplemental material); they were also detected in other viral regions (data not shown). Comparative analyses of leukemic cell and nonleukemic cells showed that 79% of C-to-T base substitutions were polymorphisms (Table 2). However, after G-to-T mutations, C-to-T mutations were still the most frequent mutations in ATL patients and HTLV-1 carriers.

Expression of the *hA3G* gene and activation-induced deaminase gene. In order to analyze the correlation between G-to-A mutation and *hA3G* expression, we first studied the mRNA level of *hA3G* using a real-time PCR assay. The *hA3G* gene was expressed in normal T cells, and the level of expression of *hA3G* moderately decreased in ATL cells. In ATL samples, there was no obvious correlation between the level of expression of the *hA3G* gene and the number of G-to-A mutations in the proviral genome.

Although only 21% of C-to-T base substitutions were mutations (Table 2), C-to-T mutations were the second most frequent mutation (see Table S2 in the supplemental material). Activation-induced deaminase (AID) was found to be a key factor for the switch recombination of immunoglobulin (Ig), and it is also implicated in hypermutations of Ig genes (15). AID deaminates cytosine to uracil. Aberrant expression of AID driven by NF-κB activation is found in gastric cancers and hepatomas, and AID expression has been invoked to explain

TABLE 5. Mutations in the *tax* region of 10 HTLV-1 carriers

HTLV-1 carrier (no. of clones)[a]	No. of the following single-nucleotide substitution in HTLV-1 carrier:								No. of sequences with the following sequence context for the G-to-A mutation[b]:			
	G-to-A	C-to-T	A-to-G	A-to-C	C-to-A	G-to-C	G-to-T	T-to-A	GA	GC	GT	GG
C72 (24)	3								1			2
C79 (24)	2	4		2	1	1					2	
C63 (21)	19											19
C40 (21)	2											2
C32 (25)	4	1										4
C62 (27)	5	1								1		4
C87 (24)	1	1							1			
C5 (26)	2											2
C29 (25)	3		3					1				3
C82 (22)	5						1					5
Total	46	7	3	2	1	1	1	1	2	1	2	41

[a] The number of clones studied from each carrier is shown in parentheses.
[b] Mutated bases are underlined.

TABLE 6. Nonsense mutations in 10 HTLV-1 carriers

HTLV-1 carrier	No. of nonsense mutations[a] in the indicated gene and position in HTLV-1 carrier:														
	pol		*env*						*p12*	*p30/p13* at 7361	*p27*[b]		*tax*		*HBZ*
	3955	4540	5465	6158	6342	6362	6482	6494			7652	7660	7469	8045	
C72	**1/25**	0/25	0/23	0/23	0/23	0/23	0/23	0/23	0/31	0/31	0/31	0/31	**1/24**	0/24	0/31
C79	**2/20**	**2/20**	0/20	0/20	0/20	**1/20**	0/20	0/20	0/24	0/24	0/24	0/24	**1/24**	0/24	0/24
C63	0/28	0/28	0/20	0/20	0/20	0/20	0/20	0/20	0/24	**2/24**	0/24	0/24	**9/21**	0/21	0/24
C40	0/26	**13/26**	0/22	0/22	0/22	0/22	0/22	0/22	0/30	0/30	0/30	0/30	**2/21**	0/21	0/30
C32	0/22	0/22	0/22	0/22	0/22	0/22	0/22	0/22	0/32	0/32	0/32	**1/32**	0/25	0/25	0/32
C62	**1/22**	0/22	0/25	0/25	**2/25**	0/25	0/25	0/25	0/28	**1/28**	0/28	0/28	**1/27**	0/27	0/28
C87	**1/22**	**3/22**	0/20	0/20	0/20	0/20	0/20	0/20	0/21	0/21	**1/21**	0/21	0/24	0/24	0/21
C5	0/22	**19/22**	0/20	0/20	0/20	**1/20**	0/20	0/20	0/24	0/24	0/24	**1/24**	**1/26**	0/26	0/24
C29	0/25	**3/25**	0/20	**1/20**	0/20	0/20	0/20	**1/20**	0/24	**2/24**	**5/24**	0/24	**1/25**	0/25	0/24
C82	**3/27**	**2/27**	**1/20**	0/20	0/20	0/20	**1/20**	0/20	0/24	**1/24**	0/24	0/24	**1/22**	**1/22**	0/24

[a] Each entry *A*/*B* in the table shows the number of clones harboring nonsense mutations at a given nucleotide position from a given carrier (*A*) along with the number of clones analyzed in that region from that carrier (*B*). The boldface values indicate that a nonsense mutation was found.
[b] Sequences of exon 2 were determined.

induced mutations observed in cancer cells (28). Therefore, we studied *AID* expression in 7 ATL cases with different proviral mutation frequencies. As shown in Fig. 4, the *AID* gene transcription increased in ATL-15. In this case, we found six C-to-T mutations in the provirus, and the sequence context showed more AID preferred sequences in C-to-T mutated sites compared to other cases without AID activation (data not shown). Thus, AID might also play a role in the deamination of the HTLV-1 genome in at least some ATL cases. Since AID is thought to target the double-stranded DNA of provirus, it likely generates C-to-T mutations in the plus strand of the provirus. However, C-to-T base substitutions contained many polymorphisms, as shown in Table 2. Therefore, correlation between C-to-T mutations and AID expression remains to be studied.

***In vitro* editing of the HTLV-1 genome by hA3G.** Previous reports have suggested that HTLV-1 is relatively resistant to the antiviral effect of hA3G (4), consistent with our finding that the frequency of G-to-A mutations throughout the HTLV-1 proviral genome was low. In order to provide direct evidence that G-to-A mutations observed in the proviruses are the result of hA3G-mediated genome editing, we studied the editing effect of hA3G on the HTLV-1 genome *in vitro*. HTLV-1 viruses were generated in the presence of exogenous hA3G to allow packaging into budding viral particles, a step that is required for exerting editing activity of the cytidine deaminase. After a round of virus infection, the HTLV-1 DNA was analyzed using a highly sensitive PCR-based protocol, referred to as 3D PCR, that is capable of amplifying G-to-A hypermutated genomes as described in Materials and Methods. Differential amplification of a *tax* region from cells infected with viral particles produced in the presence of hA3G was achieved when the denaturation PCR temperature was lowered to between 84 and 86°C (data not shown). All sequences of differentially amplified PCR clones exhibited extensive G-to-A hypermutation, and the number of G-to-A transitions ranged from 8 (13%) to 29 (48%) per clone (Fig. 5). In ATL cases and in the same region, G-to-A mutations at four nucleotide positions resulted in premature stop codons in the *p30* and *tax* genes (Fig. 1). The occurrence of such mutations was observed *in vitro* when viruses were produced together with hA3G. G-to-A

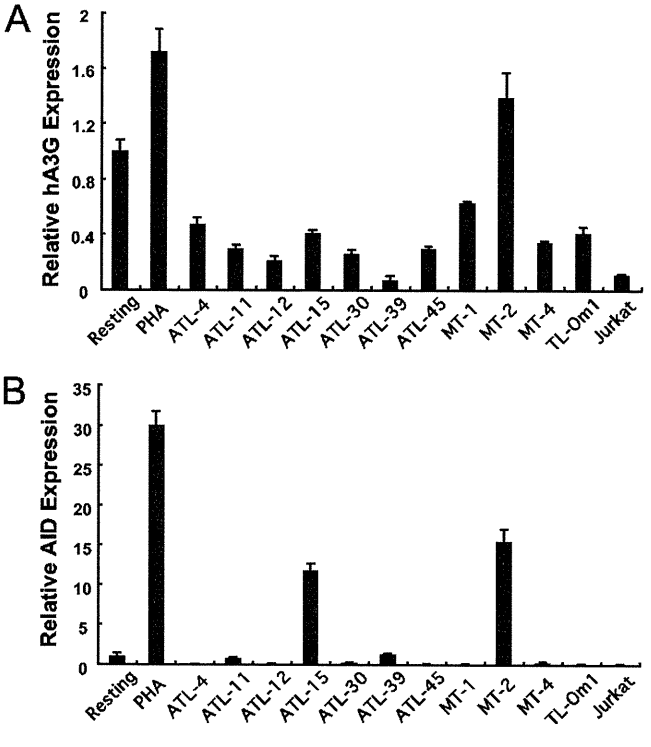

C

	G-A	C-T	A-G	T-C	A-C	A-T	C-A	C-G	T-G	Total
ATL-4	3(0)	4(1)	1			2				10
ATL-11	6(1)	9(1)	3	8		1				27
ATL-12	8(2)	8(1)	4	3				2		25
ATL-15	10(3)	6(2)	2	2	1	1			1	23
ATL-30	2(0)	1(0)				1				4
ATL-39	2(0)	8(0)	2	5	3	1				21
ATL-45	3(0)	3(0)	4	2		3	1			16

FIG. 4. Expression of the *hA3G* and *AID* genes in ATL cases and in HTLV-1-associated cell lines. Expression of the *hA3G* gene (A) and *AID* gene (B) was investigated by real-time PCR. Normal resting T cells isolated from 3 healthy blood donors were used as a control. *ACTN* was used as an internal control. Relative quantification was performed using a comparative C_T method (Applied Biosystems). Expression of *hA3G* and *AID* in resting T cells was artificially set at 1. (C) Number of nucleotide mutations in the 7 ATL cases. Among mutated sites, the number of AID-preferred sites is shown in parentheses.

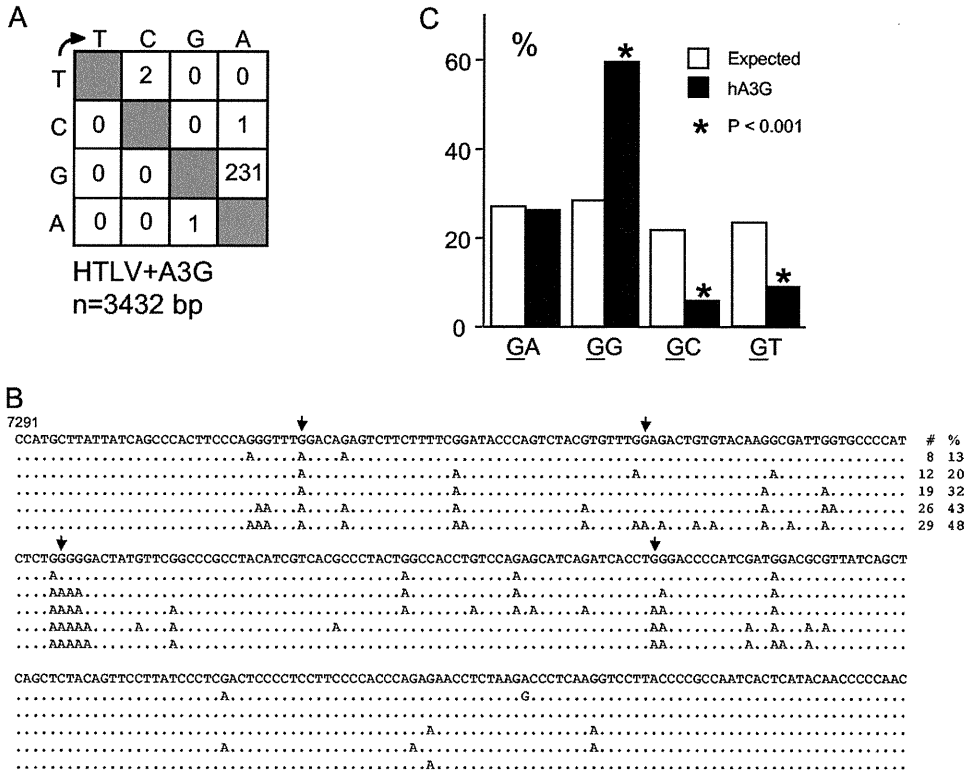

FIG. 5. *In vitro* editing of the HTLV-1 genome by hA3G. (A) Mutation matrix for hyperedited *tax* gene sequences derived from cloned 86°C 3D PCR products. The number of bases sequenced (n) is shown. (B) Hypermutated *tax* sequences from five representative PCR clones. The sequence is given with respect to the viral plus strand. Only differences from the viral plus strand are shown. The number (#) and percentage (%) of G-to-A mutations per clone are shown beside each sequence. The base composition of the sequence is 75 T (24%), 113 C (36.2%), 60 G (19.2%), and 64 A (20.5%). The position number of the first base is indicated above the base. Arrows indicate positions where G-to-A-mediated nonsense mutations were detected in ATL cases. (C) Bulk dinucleotide context of HTLV *tax* region DNA strand by hA3G. The substitution frequency as a function of the 3′ nucleotide is shown on the *y* axis. Mutated G residues are underlined. A χ^2 analysis showed that the observed frequencies by hA3G deviated significantly from the expected values ($P < 0.001$).

mutations at two sites where nonsense mutations were more frequently detected in ATL cases were also frequent among 3D PCR clones. As expected, a preference for GG dinucleotide context in hA3G-mediated G-to-A editing was observed (Fig. 5C). Our data suggested that hA3G is indeed able to actively deaminate the HTLV-1 genome during reverse transcription although with low editing frequency, leading to G-to-A mutations in the plus strand of the provirus.

DISCUSSION

In this study, in order to acquire a full mutation spectrum of HTLV-1 virus, the sequences of proviral genomes were determined in 60 ATL cases as well as 10 asymptomatic carriers. In addition to deletions and insertions, we identified base substitutions and found that G-to-A mutations were the most prevalent. In addition to the observation that G-to-A mutations in ATL patients and carriers occurred at the preferred target sequence of hA3G, we also experimentally confirmed that hA3G actively introduced G-to-A mutations to the HTLV-1 viral genome. It has been reported that hypermutation in the HTLV-1 genome was a rare event (35) and that HTLV-1 was relatively resistant to the antiviral activity of hA3G (33). Unlike HIV, which counteracts hA3G by producing Vif, HTLV-1 does not express an accessory protein that interferes with hA3G. A peptide motif in the C terminus of the HTLV-1 nucleocapsid has been shown to inhibit hA3G packaging into nascent virions (4). However, inhibition of hA3G-induced G-to-A mutations by HTLV-1 was partial (37). Previous studies analyzed small regions of provirus amplified by PCR in carriers or HAM/TSP patients, while proviral sequences of ATL cells were determined by direct sequencing. Since previous studies used error-prone *Taq* polymerase, it was very difficult to identify mutations after cloning (36). The number of ATL cases was so limited in the previous studies that mutations could not be distinguished from polymorphisms (34). This study first analyzed the entire sequence of the HTLV-1 provirus from 60 ATL cases by direct sequencing and also determined the proviral sequences of clones derived from HTLV-1 carriers using a precise DNA polymerase, which enabled us to identify mutations in HTLV-1 genomes. Consistent with previous studies (34, 35), our results showed that mutations were relatively rare. However, among the rare mutations in HTLV-1 genomes, G-to-A mutations in the target sequences of hA3G were predominant. In addition to G-to-A mutations, other mutations were also observed in ATL patients and carriers, indicating the role of other deaminases including AID and error-prone reverse transcriptase (27).

This study demonstrated important roles for cytidine deami-

nase(s) in generating mutations in HTLV-1 proviruses. So far, at least 12 cytidine deaminases have been identified, many of which share significant sequence homology. They are thought to have evolved through gene transpositions and duplications (45). Although some cytidine deaminases, including APOBEC1 and AID, target cellular genes, most human APOBEC proteins are thought to defend the host against retroviruses. Our study suggests that hA3G is responsible for G-to-A mutations in HTLV-1. hA3G binds to single-stranded DNA and preferentially deaminates CCCA and CCCG sequences during reverse transcription (48). This strategy of hA3G can induce nonsense mutations in the plus-strand coding sequence, since TGG is a target of hA3G, resulting in nonsense mutations like TAG or TGA. However, the *HBZ* gene is encoded by the minus strand of the provirus. The *HBZ* gene is therefore much less susceptible to nonsense mutations generated by hA3G. Furthermore, there are few target sequences for hA3G in the plus strand of the *HBZ* coding RNA. In addition, the coding sequence of the *HBZ* gene overlaps that of the *p12* gene. Thus, HBZ further avoids missense mutation in the minus strand.

The frequencies of G-to-A changes in the HTLV-1 provirus (0.21% for the *pol* gene and 0.11% for the *tax* gene) in the carriers are slightly lower than that for Vif-positive HIV-1 (0.57%) (48), indicating that HTLV-1 is resistant to hA3G during reverse transcription. Why are the few nonsense mutations that do occur retained in the HTLV-1 provirus? The difference between HTLV-1 and HIV-1 is related to their distinct strategies of propagation. HIV-1 replicates vigorously *in vivo*, producing tremendous numbers of viral particles. Viruses with nonsense mutations cannot replicate and thereby disappear *in vivo*. On the other hand, HTLV-1 promotes the proliferation of the infected cells themselves by the action of its regulatory and accessory genes. Therefore, HTLV-1-infected cells can proliferate despite nonsense mutations occurring in most of the viral genes, provided the cells retain the minimum set of viral genes that relate to proliferation. This might be a reason why so many nonsense mutations in various viral genes remain in the provirus. The only gene with no nonsense mutations is *HBZ*. It is likely that the *HBZ* gene is indispensable for proliferation of ATL cells, as our previous study reported (38).

Previous studies suggest that Tax is critical for proliferation of HTLV-1-infected cells and oncogenesis. However, we reported that Tax expression is frequently disrupted by three mechanisms (29). It has been speculated that Tax expression is not necessary in the late stages of ATL. Rather, since Tax is a major target of CTLs, ATL cells without Tax expression are selected during leukemogenesis. However, as shown in this study, nonsense mutations were likely generated by hA3G during reverse transcription, indicating that Tax expression was not necessary even in the carrier state. In one carrier, 9 of 21 clones shared a nonsense mutation in the *tax* gene, demonstrating clonal expansion of HTLV-1-infected cells with this mutation (see Table S5 in the supplemental material). Furthermore, 7 of 60 ATL cases contained nonsense mutations in the *tax* gene. HTLV-1-infected cells with nonsense mutations could proliferate *in vivo* and be transformed to ATL cells. A nonsense mutation in the *tax* gene has been detected in asymptomatic carriers (8). This study suggests that this nonsense mutation was generated by hA3G during reverse transcription. Another explanation is that loss of the expression of some viral gene(s) by nonsense mutations benefits the cells. Tax generates DNA damage that activates checkpoints (16, 22). In addition, it has been reported that HTLV-1-infected cells become cell cycle arrested due to the activity of Tax (19, 23). Therefore, HTLV-1-infected cells with nonsense mutations in the *tax* gene might have a growth advantage by losing Tax expression. We previously reported that HTLV-1 provirus lacking the 5′LTR and the second exon of the *tax* gene was detected in ATL cases. By sequencing the integration sites in such defective provirus, we found short 6-bp repeats generated by integrase. This finding showed that defective proviruses that could not produce Tax were generated before integration (31). Taken together, these findings indicate that Tax is not necessary for oncogenesis at least in some ATL cases.

This study suggests that nonsense mutations in the HTLV-1 provirus are generated by hA3G in both ATL cases and HTLV-1 carriers. The fact that hA3G targets the minus strand during reverse transcription explains why the *HBZ* gene is not susceptible to such nonsense mutations. In contrast, HTLV-1-infected cells take advantage of hA3G to escape from the host immune system by losing expression of other viral proteins, while the *HBZ* gene remains intact.

ACKNOWLEDGMENTS

We thank Kuan-Teh Jeang for helpful discussions, Aaron Coutts for valuable suggestions and kindly revising the manuscript, and David Derse for providing pX1MT-M.

This study was supported by a Grant-in-Aid for Scientific Research from the Ministry of Education, Science, Sports, and Culture of Japan, a grant from the Naito Foundation, and a grant from the Sumitomo Foundation to M.M. and by a grant from the Japan Leukemia Research Fund to Y.S. Y.S. is supported by JSPS Research Fellowships for Young Scientists.

REFERENCES

1. **Akagi, T., H. Ono, and K. Shimotohno.** 1995. Characterization of T cells immortalized by Tax1 of human T-cell leukemia virus type 1. Blood **86:**4243–4249.
2. **Cen, S., F. Guo, M. Niu, J. Saadatmand, J. Deflassieux, and L. Kleiman.** 2004. The interaction between HIV-1 Gag and APOBEC3G. J. Biol. Chem. **279:**33177–33184.
3. **Chiu, Y. L., and W. C. Greene.** 2008. The APOBEC3 cytidine deaminases: an innate defensive network opposing exogenous retroviruses and endogenous retroelements. Annu. Rev. Immunol. **26:**317–353.
4. **Derse, D., S. A. Hill, G. Princler, P. Lloyd, and G. Heidecker.** 2007. Resistance of human T cell leukemia virus type 1 to APOBEC3G restriction is mediated by elements in nucleocapsid. Proc. Natl. Acad. Sci. U. S. A. **104:**2915–2920.
5. **Etoh, K., S. Tamiya, K. Yamaguchi, A. Okayama, H. Tsubouchi, T. Ideta, N. Mueller, K. Takatsuki, and M. Matsuoka.** 1997. Persistent clonal proliferation of human T-lymphotropic virus type I-infected cells in vivo. Cancer Res. **57:**4862–4867.
6. **Franchini, G., R. Fukumoto, and J. R. Fullen.** 2003. T-cell control by human T-cell leukemia/lymphoma virus type 1. Int. J. Hematol. **78:**280–296.
7. **Furukawa, Y., R. Kubota, M. Tara, S. Izumo, and M. Osame.** 2001. Existence of escape mutant in HTLV-I tax during the development of adult T-cell leukemia. Blood **97:**987–993.
8. **Furukawa, Y., M. Tara, S. Izumo, K. Arimura, and M. Osame.** 2006. HTLV-I viral escape and host genetic changes in the development of adult T cell leukemia. Int. J. Cancer **118:**381–387.
9. **Gallo, R. C.** 2005. The discovery of the first human retrovirus: HTLV-1 and HTLV-2. Retrovirology **2:**17.
10. **Gaudray, G., F. Gachon, J. Basbous, M. Biard-Piechaczyk, C. Devaux, and J. M. Mesnard.** 2002. The complementary strand of the human T-cell leukemia virus type 1 RNA genome encodes a bZIP transcription factor that down-regulates viral transcription. J. Virol. **76:**12813–12822.
11. **Grassmann, R., C. Dengler, I. Muller-Fleckenstein, B. Fleckenstein, K. McGuire, M. C. Dokhelar, J. G. Sodroski, and W. A. Haseltine.** 1989. Transformation to continuous growth of primary human T lymphocytes by human

T-cell leukemia virus type I X-region genes transduced by a herpesvirus saimiri vector. Proc. Natl. Acad. Sci. U. S. A. **86:**3351–3355.
12. **Grossman, W. J., J. T. Kimata, F. H. Wong, M. Zutter, T. J. Ley, and L. Ratner.** 1995. Development of leukemia in mice transgenic for the tax gene of human T-cell leukemia virus type I. Proc. Natl. Acad. Sci. U. S. A. **92:**1057–1061.
13. **Harris, R. S., and M. T. Liddament.** 2004. Retroviral restriction by APOBEC proteins. Nat. Rev. Immunol. **4:**868–877.
14. **Hasegawa, H., H. Sawa, M. J. Lewis, Y. Orba, N. Sheehy, Y. Yamamoto, T. Ichinohe, Y. Tsunetsugu-Yokota, H. Katano, H. Takahashi, J. Matsuda, T. Sata, T. Kurata, K. Nagashima, and W. W. Hall.** 2006. Thymus-derived leukemia-lymphoma in mice transgenic for the Tax gene of human T-lymphotropic virus type I. Nat. Med. **12:**466–472.
15. **Honjo, T., H. Nagaoka, R. Shinkura, and M. Muramatsu.** 2005. AID to overcome the limitations of genomic information. Nat. Immunol. **6:**655–661.
16. **Jin, D. Y., F. Spencer, and K. T. Jeang.** 1998. Human T cell leukemia virus type 1 oncoprotein Tax targets the human mitotic checkpoint protein MAD1. Cell **93:**81–91.
17. **Kannagi, M., S. Harada, I. Maruyama, H. Inoko, H. Igarashi, G. Kuwashima, S. Sato, M. Morita, M. Kidokoro, M. Sugimoto, et al.** 1991. Predominant recognition of human T cell leukemia virus type I (HTLV-I) pX gene products by human CD8+ cytotoxic T cells directed against HTLV-I-infected cells. Int. Immunol. **3:**761–767.
18. **Koiwa, T., A. Hamano-Usami, T. Ishida, A. Okayama, K. Yamaguchi, S. Kamihira, and T. Watanabe.** 2002. 5′-long terminal repeat-selective CpG methylation of latent human T-cell leukemia virus type 1 provirus in vitro and in vivo. J. Virol. **76:**9389–9397.
19. **Kuo, Y. L., and C. Z. Giam.** 2006. Activation of the anaphase promoting complex by HTLV-1 tax leads to senescence. EMBO J. **25:**1741–1752.
20. **Lairmore, M. D., L. Silverman, and L. Ratner.** 2005. Animal models for human T-lymphotropic virus type 1 (HTLV-1) infection and transformation. Oncogene **24:**6005–6015.
21. **Liddament, M. T., W. L. Brown, A. J. Schumacher, and R. S. Harris.** 2004. APOBEC3F properties and hypermutation preferences indicate activity against HIV-1 in vivo. Curr. Biol. **14:**1385–1391.
22. **Liu, B., S. Hong, Z. Tang, H. Yu, and C. Z. Giam.** 2005. HTLV-I Tax directly binds the Cdc20-associated anaphase-promoting complex and activates it ahead of schedule. Proc. Natl. Acad. Sci. U. S. A. **102:**63–68.
23. **Liu, M., L. Yang, L. Zhang, B. Liu, R. Merling, Z. Xia, and C. Z. Giam.** 2008. Human T-cell leukemia virus type 1 infection leads to arrest in the G_1 phase of the cell cycle. J. Virol. **82:**8442–8455.
24. **Luo, K., B. Liu, Z. Xiao, Y. Yu, X. Yu, R. Gorelick, and X. F. Yu.** 2004. Amino-terminal region of the human immunodeficiency virus type 1 nucleocapsid is required for human APOBEC3G packaging. J. Virol. **78:**11841–11852.
25. **Mahieux, R., R. Suspene, F. Delebecque, M. Henry, O. Schwartz, S. Wain-Hobson, and J. P. Vartanian.** 2005. Extensive editing of a small fraction of human T-cell leukemia virus type 1 genomes by four APOBEC3 cytidine deaminases. J. Gen. Virol. **86:**2489–2494.
26. **Malim, M. H., and M. Emerman.** 2008. HIV-1 accessory proteins–ensuring viral survival in a hostile environment. Cell Host Microbe **3:**388–398.
27. **Mansky, L. M.** 2000. In vivo analysis of human T-cell leukemia virus type 1 reverse transcription accuracy. J. Virol. **74:**9525–9531.
28. **Matsumoto, Y., H. Marusawa, K. Kinoshita, Y. Endo, T. Kou, T. Morisawa, T. Azuma, I. M. Okazaki, T. Honjo, and T. Chiba.** 2007. Helicobacter pylori infection triggers aberrant expression of activation-induced cytidine deaminase in gastric epithelium. Nat. Med. **13:**470–476.
29. **Matsuoka, M., and K. T. Jeang.** 2007. Human T-cell leukaemia virus type 1 (HTLV-1) infectivity and cellular transformation. Nat. Rev. Cancer **7:**270–280.
30. **Mitchell, M. S., E. T. Bodine, S. Hill, G. Princler, P. Lloyd, H. Mitsuya, M. Matsuoka, and D. Derse.** 2007. Phenotypic and genotypic comparisons of human T-cell leukemia virus type 1 reverse transcriptases from infected T-cell lines and patient samples. J. Virol. **81:**4422–4428.
31. **Miyazaki, M., J. Yasunaga, Y. Taniguchi, S. Tamiya, T. Nakahata, and M. Matsuoka.** 2007. Preferential selection of human T-cell leukemia virus type 1 provirus lacking the 5′ long terminal repeat during oncogenesis. J. Virol. **81:**5714–5723.
32. **Miyazato, P., J. Yasunaga, Y. Taniguchi, Y. Koyanagi, H. Mitsuya, and M. Matsuoka.** 2006. De novo human T-cell leukemia virus type 1 infection of human lymphocytes in NOD-SCID, common gamma-chain knockout mice. J. Virol. **80:**10683–10691.
33. **Navarro, F., B. Bollman, H. Chen, R. Konig, Q. Yu, K. Chiles, and N. R. Landau.** 2005. Complementary function of the two catalytic domains of APOBEC3G. Virology **333:**374–386.
34. **Okazaki, S., R. Moriuchi, N. Yosizuka, K. Sugahara, T. Maeda, I. Jinnai, M. Tomonaga, S. Kamihira, and S. Katamine.** 2001. HTLV-1 proviruses encoding non-functional TAX in adult T-cell leukemia. Virus Genes **23:**123–135.
35. **Renjifo, B., I. Borrero, and M. Essex.** 1995. Tax mutation associated with tropical spastic paraparesis/human T-cell leukemia virus type I-associated myelopathy. J. Virol. **69:**2611–2616.
36. **Saito, M., Y. Furukawa, R. Kubota, K. Usuku, S. Sonoda, S. Izumo, M. Osame, and M. Yoshida.** 1995. Frequent mutation in pX region of HTLV-1 is observed in HAM/TSP patients, but is not specifically associated with the central nervous system lesions. J. Neurovirol. **1:**286–294.
37. **Sasada, A., A. Takaori-Kondo, K. Shirakawa, M. Kobayashi, A. Abudu, M. Hishizawa, K. Imada, Y. Tanaka, and T. Uchiyama.** 2005. APOBEC3G targets human T-cell leukemia virus type 1. Retrovirology **2:**32.
38. **Satou, Y., J. Yasunaga, M. Yoshida, and M. Matsuoka.** 2006. HTLV-I basic leucine zipper factor gene mRNA supports proliferation of adult T cell leukemia cells. Proc. Natl. Acad. Sci. U. S. A. **103:**720–725.
39. **Sheehy, A. M., N. C. Gaddis, and M. H. Malim.** 2003. The antiretroviral enzyme APOBEC3G is degraded by the proteasome in response to HIV-1 Vif. Nat. Med. **9:**1404–1407.
40. **Takatsuki, K.** 2005. Discovery of adult T-cell leukemia. Retrovirology **2:**16.
41. **Takeda, S., M. Maeda, S. Morikawa, Y. Taniguchi, J. Yasunaga, K. Nosaka, Y. Tanaka, and M. Matsuoka.** 2004. Genetic and epigenetic inactivation of tax gene in adult T-cell leukemia cells. Int. J. Cancer **109:**559–567.
42. **Tamiya, S., M. Matsuoka, K. Etoh, T. Watanabe, S. Kamihira, K. Yamaguchi, and K. Takatsuki.** 1996. Two types of defective human T-lymphotropic virus type I provirus in adult T-cell leukemia. Blood **88:**3065–3073.
43. **Taniguchi, Y., K. Nosaka, J. Yasunaga, M. Maeda, N. Mueller, A. Okayama, and M. Matsuoka.** 2005. Silencing of human T-cell leukemia virus type I gene transcription by epigenetic mechanisms. Retrovirology **2:**64.
44. **Trono, D.** 2004. Retroviruses under editing crossfire: a second member of the human APOBEC3 family is a Vif-blockable innate antiretroviral factor. EMBO Rep. **5:**679–680.
45. **Turelli, P., and D. Trono.** 2005. Editing at the crossroad of innate and adaptive immunity. Science **307:**1061–1065.
46. **Wiegand, H. L., B. P. Doehle, H. P. Bogerd, and B. R. Cullen.** 2004. A second human antiretroviral factor, APOBEC3F, is suppressed by the HIV-1 and HIV-2 Vif proteins. EMBO J. **23:**2451–2458.
47. **Yoshida, M., Y. Satou, J. Yasunaga, J. Fujisawa, and M. Matsuoka.** 2008. Transcriptional control of spliced and unspliced human T-cell leukemia virus type 1 bZIP factor (HBZ) gene. J. Virol. **82:**9359–9368.
48. **Yu, Q., R. Konig, S. Pillai, K. Chiles, M. Kearney, S. Palmer, D. Richman, J. M. Coffin, and N. R. Landau.** 2004. Single-strand specificity of APOBEC3G accounts for minus-strand deamination of the HIV genome. Nat. Struct. Mol. Biol. **11:**435–442.
49. **Yu, X., Y. Yu, B. Liu, K. Luo, W. Kong, P. Mao, and X. F. Yu.** 2003. Induction of APOBEC3G ubiquitination and degradation by an HIV-1 Vif-Cul5-SCF complex. Science **302:**1056–1060.